Volume 11 Number 2, August 2026, pp. 222-238
P-ISSN:2477-7935
E-ISSN: 2548-6225
DOI: 10.59052/edufisika.v11i2.54088

DETERMINATION OF BOLTZMANN FACTOR IN SAE 10W-30 LUBRICANT THROUGH FALLING BALL VISCOSITY HANDS-ON APPROACH

Ngia Masta, Eki Evendi, Randi Wardani, Resmi Karmila
Pendidikan Fisika Study Program, Universitas Kristen Indonesia, Jakarta, Indonesia
Corresponding author email: ngia.masta@uki.ac.id

Article Info
Received: 27 March 2026
Accepted: 21 July 2026
Publication: 02 August 2026

Abstract :
Statistical mechanics bridges macroscopic fluid properties with microscopic molecular dynamics, yet its experimental estimation remains a challenge in physics education. To overcome this learning obstacle, Boltzmann Factor estimation could be performed with a simple Hands-on approach, one of which is the viscosity of a falling ball. This study validates the falling ball thermo-viscosity method for estimating activation energy and Boltzmann Factor in the Francis wall-correction model to resolve the wall effect with narrow tube ($\lambda = 0.69$). It uniquely applies Federal Racing Matic SAE 10W-30 oil bridging macroscopic kinetics with statistical microscopic parameters. The experiment was conducted by dropping a marble into the fluid at a fixed distance with a temperature variation between 308 K – 328 K. Compensation for the wall effect of the tube was carried out through Francis correction. Reynolds number indicated deviation from Stokes' regime, resulting in an apparent rather than true viscosity. From the plot of approximation viscosity vs invers temperature, Arrhenius Law extracted E_a value is 35.66 ± 6.35 kJ/mol. Meanwhile relative Boltzmann Factor were close to the industrial data. Pearson's r (0.97) and values of R2 (0.94) indicate high methodological validity. Despite geometric limitations causing ~25% deviation in viscosity, the temperature-dependent trend remains enabling accurate activation energy estimation and extraction of the relative Boltzmann factor. These results support the falling ball viscosity method as a simple alternative experimental approach for quantitatively visualizing the abstract theory of classical particle distributions

Keywords: Activation energy; Arrhenius law; Engine lubricant; Statistical physics; Reynold number.

This is open access article under the CC BY-SA licence

INTRODUCTION

Statistical mechanics, including the Maxwell-Boltzmann distribution function, is a fundamental pillar that bridges macroscopic phenomena with microscopic behavior (Guisasola, 2014). However, the abstraction of this concept often poses a significant cognitive barrier for students, especially in understanding probability (Hull et al., 2021). Although students are able to perform partial mathematical manipulation, they tend to have difficulty in presenting contextual applications (Koerfer, 2025). The

dominance of theoretical-mathematical approaches with minimal contextual application causes students to have difficulty visualizing how the distribution of molecular energy determines the physical properties of matter (Swendsen, 2012). This challenge is universal, as reported across various higher education institutions (M. Khan et al., 2025). Limited mastery of statistical mechanics in depth can have an impact on low mastery of advanced physics such as machine learning (Gorban & Tyukin, 2018), solid state physics (Karmakar et al., 2010) and even financial economics (Jovanovick & Schinckus, 2018), which depends on understanding the probability distribution.

To mitigate this abstraction-reality dichotomy, the Hands-on approach have been advocated in transforms statistical mechanics learning into something more contextual experience (Rosen & Kelly, 2020). This method has proven effective in overcoming learning difficulties in advanced physics courses, both in offline and online learning modes (Lang, 2012). One potential method is falling-ball viscosity experiment utilizing microcontroller-based sensors like Arduino (Bachtiar et al., 2024). While such technology improves the precision of fall time measurements, a critical conceptual "gap" remains: macroscopic terminal velocity is often directly – and inaccurately- integrated into Boltzmann distribution function without proper bridging. To accurately extracted into relevant microscopic parameters, macroscopic data must first be bridged via the Arrhenius law (Suharto., 2022). Furthermore, while activation energy (ϵ_a)studies have been widely conducted, like sea water (Brewer et al., 2021), used vegetable oil (Haryanto & Prabawa, 2016), soybean oil (Ike, 2019) to canola oil (Fasina & Colley, 2008), the empirical link between ϵ_a and Boltzmann factor remains largely confined to idealized laboratory solvent like ethanol and acetone (Fazio et al., 2012).

The novelty of this work lies in applying Federal Racing Matic SAE 10W-30 by corporate narrow tube to extract $\epsilon_a$and probability (Boltzmann factor) of particles distributions. Beyond the choice of fluid, the physical constraints of experimental setups in educational often introduce additional hydrodynamic complexities that are frequently overlooked. In many practical scenarios, such as the use of narrow cylindrical tubes to conserve fluid samples or fit within portable apparatuses, the interaction between the falling sphere and the vessel walls becomes dominant. These high ratio of ball and vessel invalidate the standard Stokesian assumptions typically taught in introductory courses. Consequently, this study aims to rigorously evaluate the validity of falling-ball thermo viscosity method in estimating Ea and Boltzmann factor by incorporate the Francis wall-correction model to resolve friction effects of narrow tube ($\lambda = 0.69$). To ensure maximum validity, a multilateral validation strategy is employed: cross-referencing experimental findings against industrial standard Technical Data Sheets (TDS), comparisons with peer-reviewed literature, an also complemented by reliability analysis and uncertainty assesments.

This approach provides a significant methodological contribution by minimizing systematic errors in falling ball viscometry while offering a robust framework for physics instructors to implement affordable and conceptually deep experiments in statistical mechanics.

RESEARCH METHOD

2.1 Research Design

This research is a quantitative experimental study. The experiment was conducted to estimate the Boltzmann factor through the thermo-viscosity of SAE 10W-30 oil fluid. Viscosity was obtained from the terminal velocity of the falling ball to be extracted into activation energy parameters and the Boltzmann factor.

2.2 Instruments, and Data Collection Techniques

The working fluid used was a commercial lubricant with the specification Federal Racing Matic SAE 10W-30. The selection of Federal Racing Matic lubricant as the object of study in this research is in line with its relatively low price, easy to obtain and has implemented molecular viscosity technology (ExxonMobil Indonesia, 2025). The test balls in this study were marbles with a diameter of 0.01725 m and a density of 2112.553 kg/m^3. Viscosity testing was carried out on a transparent cylindrical tube with a diameter of 0.025 m. The ratio of the ball diameter to the tube diameter was λ of 0.69. The ball's travel time was measured using a stopwatch. While oil temperature is monitored using a glass thermometer. Heating was carried out in a 500 mL measuring cylinder on a magnetic stirrer hot plate.

2.3 Research Object

This study focuses on examining the validity of using the falling ball thermo-viscosity method on a narrow cylindrical tube ($\lambda = 0.69$) in estimating the activation energy value and Boltzmann factor in Federal Racing Matic SAE 10W-30 oil. This study used the Arrhenius law to analysed the correlation between macroscopic viscosity-induced resistance and tube geometry constraints on the microscopic particle dynamics of engine oil fluids.

2.4 Data and Sample Characteristic

The research data is quantitative experimental in nature, obtained from measuring the ball's fall time (t) on the Federal Racing Matic SAE 10W-30 oil sample. The travel time data obtained is then converted into a dynamic viscosity value (η) and transformed into natural logarithms ($\ln \eta$) for linearity analysis using the Arrhenius model. This study emphasized the robustness of the thermoviscous trend, where the slope of Arrhenius plot remains physically invariant, rather than aiming for idealized absolute numerical accuracy of viscosity, which is often unattainable in decentralized or pedagogical experimental setups.

The experimental temperature range was strategically narrowed to 308 K - 328 K in 5 K increment, to reflect typical motorcycle engine start-up conditions in tropical road environments, which are often slightly warmer than room temperature. The significantly decreased viscosity at higher temperature lubricants would shorten fall times that approach the limits of human reaction time resolution during manual stopwatch timing. Thus, temperature above 328 K were not tested due to instrument limitations, which consequently increased the relative measurement uncertainty.

However, the data quality screening has been conducted. The data at 318 K were identified as statistical outliers because they showed extreme deviations from the theoretical model of monotonic temperature-viscosity trend. As only one measurement was obtained at each temperature point, the 318 K deviation could not be confirmed through replication. This deviation could be caused by human error in time measurement, momentary thermal instability, or bubble anomalies. Therefore, these data points were excluded in Arrhenius plot to ensure the reliability (Sub Section 3.2.2).

2.5 Research Parameters

This research involved three main categories of parameters that were observed and analysed, namely:

a. Experimental Physical Parameters, which include: fall time (t) and terminal velocity of the ball (v_t) as dependent variables and fluid temperature (T) as independent variable.
b. The physical parameters analysed are ϵ_a and Boltzmann factor. Activation energy (ϵ_a) determined from the gradient of the Arrhenius plot extracted based on the relationship between $\ln \eta$ and T^{-1}. Meanwhile, the relative Boltzmann factor (P_{rel}) analysed as a representation of the probability of a particle overcoming viscous resistance at a given temperature, calculated based on the obtained ϵ_a value.
c. Statistical Validation Parameters, analysed to test the validity of the model, which include Reynolds number, Pearson correlation coefficient (r), Coefficient of determination (R^2), and Residual Sum Squares (RSS).

2.6 Research Procedure

A ball is dropped vertically into a fluid at a fixed distance (s) = 10 cm (0.10 m). The ball's falling speed is calculated using $v = s.t^{-1}$, with: v = ball velocity (m/s), and t = time of the ball fall (s) . Viscosity is measured using the falling ball method according to the following instrument scheme (Figure 1). The stages of implementing the practical work on the Study of the Effect of Temperature on Engine Oil Viscosity using Stokes' Law and Boltzmann Distribution Function are given in Figure 2.

2.7 Data Analysis Technique

2.7.1 Determination of Fluid Density

As for the density of the fluid (ρ_f) The results used in this study are extrapolation results from TDS Federal Racing Matic 10W-30 (ExxonMobil Indonesia, 2025). Extrapolation is done using the reference

oil density of SAE 10W-30 at T_{ref}= 288K is ρ_{ref}= 860 kg/m^3 according to ASTM D4052 and coefficient of thermal expansion (β) is 0.0007/°C. To obtain the density at temperature, the Eq. (1) is used:

$$\rho_f = \rho_{ref} \times \left[1 - \beta\left(T - T_{ref}\right)\right] \quad (1)$$

With: ρ_f = density at the desired temperature (kg/m^3), and T = the desired temperature (K)

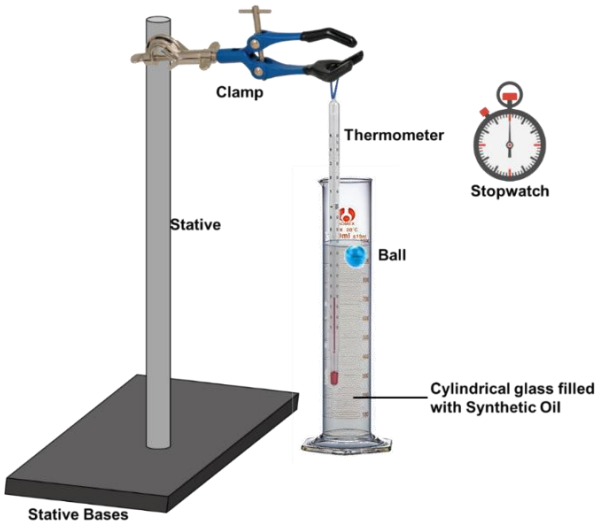

Figure 1 Instrument Schematic

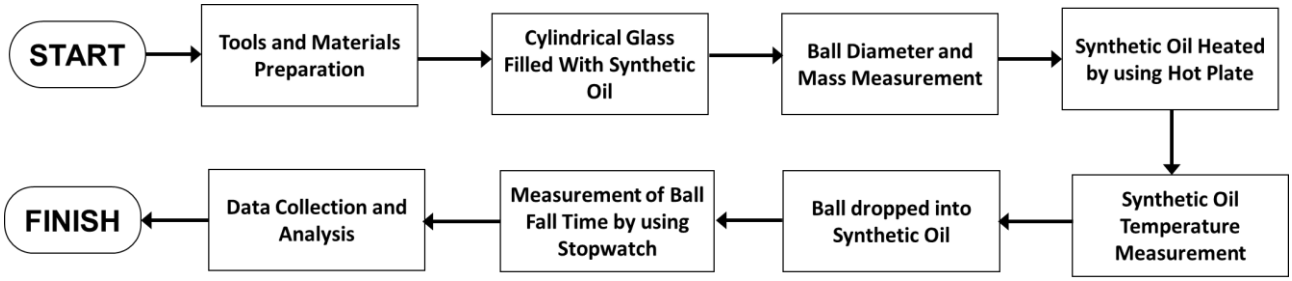

Figure 2 Research Procedure Diagram

2.7.2 Fluids Viscosity

a. Fluid Viscosity in the Falling Ball Method

Viscosity is a physical property of a fluid that indicates the level of thickness or internal resistance of the fluid to flow (Suri et al., 2023). In this study, two types of viscosity were used, namely dynamic viscosity and kinematic viscosity. Dynamic viscosity or absolute viscosity measures a fluid's resistance to flow when an external force acts on it (Chekirda et al., 2022). It is this absolute viscosity parameter that is used in the Stokes force and Francis correction. For the falling ball method, by substituting the Archimedes force and Stokes force, the dynamic viscosity is obtained by $\eta = \frac{2r^2 g(\rho_b - \rho_f)}{9v}$, with: η = dynamic viscosity ($Pa.s$), ρ_b = ball densities (kg/m^3), ρ_f = fluid densities (kg/m^3), and v = fall-ball velocity (m/s)

b. Lee and Francis Correction

In the falling ball viscosity experiment, if the diameter of the ball is not much smaller than the diameter of the tube, there will be additional drag from the tube wall (Salim, 2014). This often causes the dynamic viscosity value to be higher than the actual value (Cho et al., 1980). If the diameter of the tube is not much larger (at least ten times) than the diameter of the ball, the friction of the walls will significantly inhibit the fall of the ball, so that the oil will appear to become thicker (Ataíde et al., 1990). The absolute

viscosity after correction is generally given in Eq. (2):

$$\eta_{corrected} = \frac{\eta}{K} \tag{2}$$

With: $\eta_{corrected}$ = Viscosity value after correction (Pa.s), η = dynamic viscosity $(Pa.s)$, and $K =$ correction factor. The wall effect is influenced by the ratio of the diameter of the ball to the tube (λ), which is stated by $\lambda = \frac{d_{ball}}{d_{tube}}$. For a fairly high ratio, according to this research $\lambda = 0{,}69$ the suitable viscosity correction due to wall effects is the Lee and Francis correction (Iwaoka & Ishii, 1979). Lee's correction factor can be applied over a range of $0{,}7 \leq \lambda \leq 1$ with the large Lee correction factor given by Eq. (3):

$$K = \frac{3}{\sqrt{2}}\frac{\pi}{8}(1-\lambda)^{-\frac{5}{2}} \tag{3}$$

While the conditions for using the Francis correction factor are in the interval $\lambda \leq 0{,}832$ The magnitude of the Francis correction factor is given by Eq. (4) (Cho et al., 1980):

$$K = (1-\lambda)^{-\frac{9}{4}} \tag{4}$$

2.7.3 Activation Energy and the Arrhenius Equation

Activation energy is the minimum energy that a particle must have so that a physical or chemical process can take place (Brewer et al., 2021). In this study, activation energy is the energy required for fluid molecules to move from one to another state. This movement process plays a crucial role in determining the fluid's viscosity (Ike, 2019). The effect of temperature on the viscosity of liquid fluids can be empirically explained using the Arrhenius Equation (S. U. Khan et al., 2022). This equation states that the viscosity of a fluid decreases exponentially with increasing temperature, and is expressed in $\frac{\ln \eta}{T^{-1}} = \frac{E_a}{R} = m$, with: η = viscosity (Pa.s), $\ln \eta =$ natural logarithm of viscosity, $\epsilon_a =$ flow activation energy per molecule (J/mol), $T =$ absolute temperature (K), m = gradient value of Arrhenius plot, and the activation energy is expressed by Eq.(5)

$$\epsilon_a = m \,.\, k_B \tag{5}$$

In this study, the effect of temperature on viscosity using the falling ball method based on Stokes' Law, the viscosity values obtained at various temperatures can be analysed using the Arrhenius equation. By plotting a graph $\ln \eta$ versus $1/T$, a linear relationship with a gradient of E_a/R. From this gradient, the activation energy of the fluid can be determined experimentally (Wentao et al., 2024).

2.7.4 The Relative of Boltzmann Factor

Fluids are composed of molecules that are always moving randomly due to the thermal energy they possess and the microscopic behavior of these particles is greatly influenced by the temperature of the system (Truesdell & Rajagopal, 2000) . To describe the energy distribution of molecules in a fluid at thermal equilibrium, the Boltzmann distribution function is used, which is the basis of classical statistical physics (Shams & Mirzaie, 2025). The Boltzmann distribution function states that the probability of a molecule having energy ϵ on temperature T given by Eq. (6) (Trevor et al., 2010):

$$P_{rel} = \frac{P_T}{P_{ref}} = \exp\left(-\frac{\epsilon_a}{k_B}\right)\exp\left(\frac{1}{T} - \frac{1}{T_{ref}}\right) \tag{6}$$

With: $P_T =$ Boltzmann Factor at temperature T, $\epsilon_a =$ activation energy per molecule from the Arrhenius equation (J/mol) and $T =$ absolute temperature (K)

2.5 Data Validation

a. Testing the Validity of Stokes' Law Implementation through Reynolds Numbers

Reynolds number (Re) is calculated to ensure the validity of Stokes' Law (Bai et al., 2022). The Reynolds number equation is given by Eq. (7):

$$Re = \frac{\rho_f . v . d_{ball}}{\eta} \tag{7}$$

b. Validity Test of Activation Energy through Uncertainty

The uncertainty in the activation energy is influenced by the uncertainty in the gradient, which is obtained from the linear fitting. Error propagation is then performed to determine the uncertainty in the activation energy. The equation used to calculate the uncertainty in the activation energy is according to $\Delta\epsilon_a = \Delta m \,.\, k_B$, with: ΔE_a = Standard Error of Activation Energy (J/mol), Δm= Standard Error of Arrhenius slope and R = Ideal Gasses Constant = 8.314 K

c. Validity Evaluation of Activation Energy from Arrhenius Plot Gradient

The reliability test of the activation energy (Ea) estimate obtained from the Arrhenius law was carried out through linear regression analysis on the plot of the relationship between the natural logarithm of the reaction rate constant (ln η) against the inverse of the thermodynamic temperature (1/T). Internal consistency and linearity of the data were evaluated using the Pearson correlation coefficient r to measure the strength and direction of the linear relationship between the temperature and reaction rate variables, where a value close to -1 indicates a perfect negative correlation in accordance with the Arrhenius theoretical model (Montgomery & Runger, 2018). Next, the coefficient of determination (R^2) is applied to determine the proportion of the variance of the experimental data that can be explained by the linear model; a high R^2 value (close to 1.0) indicates a high level of precision and reliability in determining the kinetic parameters (Atkins & Paula, 2006). To validate model accuracy and minimize uncertainty, a Residual Sum of Squares (RSS) calculation is performed to measure the total deviation between the experimental data points and the predicted values on the regression line. A significantly low RSS value indicates that the Arrhenius model has an optimal fit (goodness of fit) to the experimental data with a minimal error rate (Miller & Miller, 2010).

d. Validity Test Through Reference Data

The evaluation of the validity of viscosity data, activation energy, and Boltzmann factor in this study was carried out through the integration of industry standard parameters extracted from the official Technical Data Sheet (TDS) of Federal Racing Matic 10W-30 lubricant (ExxonMobil Indonesia, 2025). The main reference data includes kinematic viscosity at 313 K and 373 K, also density at 298 K (860 kg/m^3), all of which were tested based on the ATM D445 and ASTM D1250 protocols. These values (η)were used as a baseline for calculating the reference activation energy and Boltzmann factor. The density value resulting from thermal extrapolation according to Eq. (1). The determination of the activation energy value is calculated using the linear form of the Arrhenius equation, in Eq. (8):

$$E_{a,,ref} = \frac{R \ln\left(\frac{\eta_1}{\eta_2}\right)}{\frac{1}{T_1} - \frac{1}{T_2}}, \tag{8}$$

The magnitude of dynamic viscosity at temperature T_1= 308 K and T_2= 328 K. Then, by substituting the ideal gas constant value R into equation (5), the value is obtained. $E_{a,,ref}$ = 34.90 kJ/mol.

The Technical Data Sheet (TDS) data used in this study serve as a reference; however, it should be noted that such data are typically provided for general characterization purposes and often lack detailed information regarding experimental conditions, measurement procedures, and associated uncertainties. Therefore, while TDS data are useful for preliminary validation, they may not fully represent specific experimental conditions, and additional comparison with peer-reviewed

RESULTS AND DISCUSSION

3.1 Profile of Fluids Velocity, Viscosity, and Reynolds Number

3.1.1 Trends from a Falling Ball Thermal - Viscosity Experiment

In mechanical systems, particularly in vehicle engine oil, engine oil acts as a lubricant to reduce friction and wear, and helps cool engine components. Macroscopic analysis of the thermo-viscosity profile in Figure 3 shows that the ball terminal velocity and fluid viscosity have an inverse relationship. As the fluid temperature increases, its viscosity decreases, and the ball's terminal velocity increases significantly. As illustrated in Figure 4, the comparison of viscosity values obtained from experimental measurements and correction models provides important insight into the transparent analysis. The

viscosity–temperature curves show that the experimental data consistently yield higher values than the corrected and TDS curves, with a pronounced peak at 318 K, which can be clearly identified as an outlier. This anomaly is likely caused by the measurement procedure, where the falling time was recorded manually using a stopwatch and performed as a single measurement, making it highly susceptible to human reaction time error and random fluctuations.

Furthermore, the experimental and corrected data do not fully overlap with the TDS reference, as noticeable deviations remain even after applying both Lee and Francis corrections. This indicates that the obtained viscosity values, despite correction, should be considered as approximate (apparent) values rather than exact intrinsic properties of the fluid. Nevertheless, for subsequent analysis, the Francis-corrected data are selected because they show the closest agreement with the TDS trend and provide a more consistent and systematic representation of the temperature-dependent behavior compared to the Lee correction. Therefore, the Francis-corrected data are considered the most reliable basis for further analysis, particularly in capturing the relative temperature dependence required for Reynold number and Arrhenius plot in activation energy determination.

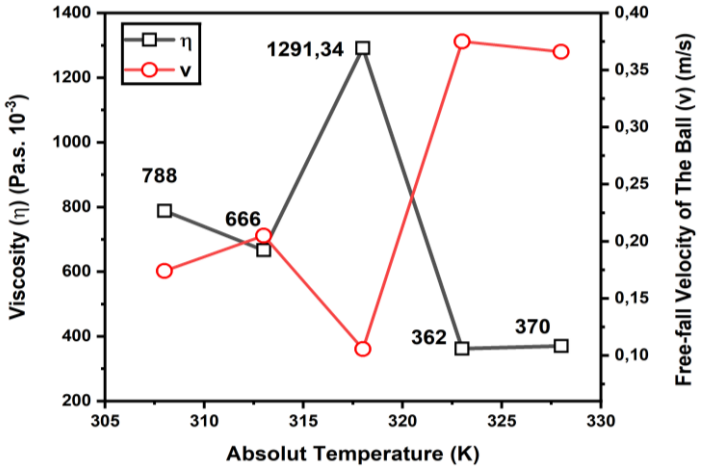

Figure 3 Comparison Diagram of Viscosity and Velocity in Temperature Variation

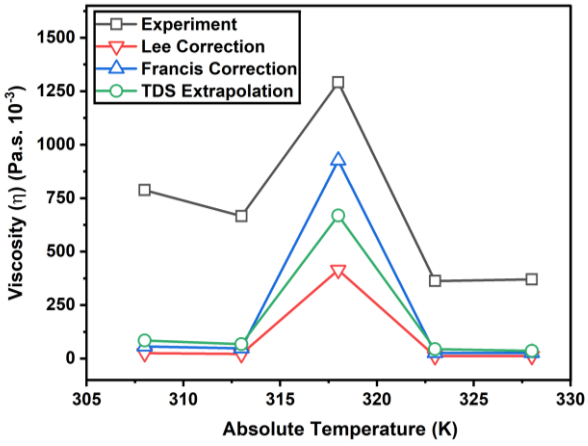

Figure 4 Evaluation of Viscosity Corrections (Lee and Francis) Against Experimental and TDS Data

3.1.2 Viscosity Validity Evaluation

a. Viscosity Correction Compared with Reference Data

To evaluate the consistency of the experimental results, the Francis-corrected viscosity values were compared with literature data at different temperatures, as presented in Table 1. At 313 K, the measured viscosity (0.048 Pa·s) shows deviations ranging from 5.88% to 42.17%, indicating partial agreement but with noticeable variability depending on the reference. As the temperature increases to 323 K, the deviation rises significantly to around 49–51%, suggesting reduced accuracy of the experimental

method at lower viscosity conditions. However, at 328 K, the deviation decreases to 10%, indicating improved agreement under specific conditions. Overall, the mean deviation of 25.76% suggests that the measured values represent an approximate viscosity rather than exact intrinsic viscosity.

This variation may be influenced by differences in experimental conditions, manual time measurement techniques and apparatus geometric limitation. These geometric limitations are primarily attributed to the high ball-to-tube ratio ($\lambda = 0.67$), indicating that the sphere occupies nearly 70% of the tube diameter, thereby inducing significant hydrodynamic confinement known as the wall effect (Celata et al., 2006). Under this condition, the surrounding fluid is strongly restricted, leading to an increase in flow resistance and an overestimation of the viscous drag compared to an unbounded medium. As a result, the measured falling velocity is reduced, which directly contributes to deviations in the calculated viscosity values relative to literature data.

Table 1 Comparison of Experimental (Francis-Corrected) and Literature Viscosity Values with Deviation Analysis

T (K)	Dynamic Viscosity of Lubricant Oil SAE 10W-30 (Pa.s)				Refference
	Francis Corr	Literature*	Deviation (Δ)*	% Δ	
313	0.048	0.067	0.019	28.36	(ExxonMobil Indonesia, 2025)
		0.083	0.035	42.17	(Canciam, 2012)
		0.063	0.015	23.81	(Abed et al., 2024)
		0.060	0.012	20.00	(Hei et al., 2023)
		0.059	0.011	18.64	(Calabokis et al., 2022)
		0.058	0.010	17.24	(Puspitasari et al., 2024)
		0.058	0.010	17.24	(Mushtaq & Hanief, 2021)
		0.051	0.003	5.88	(Taha et al., 2024)
323	0.026	0.053	0.027	50.94	(Canciam, 2012)
		0.051	0.025	49.02	(Puspitasari et al., 2024)
328	0.027	0.030	0.003	10.00	(Hei et al., 2023)
Mean Deviation (%)				25.76	

*Approximation value

Although the viscosity values have been corrected using the Francis correction to account for wall effects, noticeable deviations from literature data still persist. This indicates that the discrepancies are not solely caused by geometric confinement, but also by the limitations of the correction model itself (Ashley et al., 2024). The Francis correction does not account for changes in flow structure around the sphere, such as local velocity gradients, end effect and/ or evolving wake behavior, which influence the effective drag experienced by the particle (Zanoun et al., 2025). As a result, even after correction, the measured viscosity values remain slightly overestimated relative to literature data. Though the Francis-corrected viscosity values still deviate from absolute accuracy, the present analysis is based on the temperature-dependent trend rather than the exact magnitude (Xue et al., 2022). This is justified because the estimation of activation energy and the Boltzmann factor depends on the relative change in viscosity with temperature, making the trend a physically meaningful and reliable basis for interpretation (Hamdi & Mliki, 2023).

3.1.4 Reynolds Value Profile

The Reynolds number, which calculated by Eq.7), is used to confirm the type of fluid flow required to validate the suitability of Stokes' Law in this experiment. The Reynolds number as shown in Table 2, confirms the deviation from Stokes Law. Since creeping flow assumption underlying Stokes' law at $Re << 1$ (Rhodes & Seville, 2024). The Re number varies from 24 to 303, which indicates that the flow is still considered laminar, but flow separation, wake and vortex have been formed behind the ball (Schlichting & Gersten, 2017). At Re = 24 – 91, flow separation emerges and develops into an oscillating ring eddy, with the drag coefficient progressively deviating from and ultimately losing correlation with Stokes predictions (Southard, 2019). At higher values, Re = 288 and 303, vortex rings are periodically shed into the wake and decay downstream as new structures form, accompanied by the onset of turbulence.

These observations indicate that inertial and unsteady wake effects dominate the flow behavior, confirming that the creeping flow assumption underlying Stokes' law is no longer valid. Although Stokes'

law was employed to estimate viscosity, the calculated viscosity also confirmed as an approximation viscosity rather than an exact intrinsic property. The limitation of the Stokes-based approach under moderate Reynolds number conditions highlights the need for an alternative theoretical perspective to explain fluid resistance. In such regimes, viscous behavior is not solely governed by macroscopic drag forces but also by microscopic molecular interactions and energy barriers.

Table 2 Fluid Flow Type Based on Reynold Number

T (K)	Reynold Number (Re)	Interpretation of Flow Characteristic	
		(Schlichting & Gersten, 2017)	(Southard, 2019)
308	65	Laminar with unstable wake and karman vortex street	Flow separation develops and forms a Eddy's ring behind the sphere, which becomes increasingly unstable and oscillated. The rising of Reynolds number leads to cyclic detachment (vortex shedding)
313	91		
318	24		
323	303	Laminar with vortex street instabilities	
328	288		Pressure forces dominate over viscous effects, with turbulence emerging in the wake region.

3.2 Activation Energy

3.2.1 Validity Evaluation of the Activation Energy of the Arrhenius Law

The validity of the activation energy analysis methodology using the Arrhenius law was evaluated based on Pearson's r value, coefficient of determination (R^2), and Residual Sum Square (RSS). For transparency, the complete dataset (308 K – 328 K) is shown in Figures 3 and 4. In the Arrhenius analysis (Figure 5), the 318 K observation was excluded because it was inconsistent with the expected temperature–viscosity pattern and reduced the statistical reliability of the fitted trend. To quantify the impact of this decision, we repeated the analysis under inclusion versus exclusion of the 318 K observation, and we report the resulting fit metrics below (Table 3).

Table 3 Validity test Based on Linear Correlation From Arrhenius Plot

Parameter		Pearson's r	R^2	RSS	Detail
Value	Including 318 K data	0.62	0.38	0.72	Not used in the Arrhenius Plot
	Excluding 318 K data	0.97	0.94	0.03	Used in the Arrhenius Plot

A sensitivity analysis was conducted by refitting the model with and without the 318 K observation. Excluding 318 K markedly improved model fit (R^2 increased from 0.38 to 0.94; RSS decreased from 0.72 to 0.03). Notably, the strength of the linear association increased substantially when 318 K was excluded, as indicated by Pearson's correlation increased from 0.62 (with 318 K) to 0.97 (without 318 K), indicating a much stronger linear association after exclusion.), consistent with a markedly improved fit and reduced residual error. This indicates that the 318 K point primarily introduced excess residual error rather than changing the underlying relationship.

Pearson's r value (0.97) indicates a strong positive correlation between the inverse of T and ln η. Statistically, this value validates the thermo-viscosity relationship in SAE 10W-30 oil according to a linear trend on a logarithmic scale. As for the coefficient of determination R^2 = 0.94 showed 94% variations in oil viscosity can be explained by consistently observed temperature changes. In pure laboratory studies, the values R^2 expected to be R^2>0.95. However, for a hands-on approach with simple tools, a value of 0.94 is sufficient to indicate a physical phenomenon, although it still indicates the presence of noise or experimental uncertainty. Furthermore, the goodness of fit of the R^2 value shows the thermo-viscosity trend successfully recorded through the hands-on approach of falling ball viscosity, which is simple, capable of determining microscopic molecular activation energies. Meanwhile, the Residual Sum of Squares (RSS = 0.03) value shows a fairly small value, which indicates that the deviation of the data from the best-fit line is not too extreme.

3.2.2 Arrhenius Plot

The observation data at 318 K was excluded due to data screening, as we mention in section 2.4. The slope resulting from the linear fitting of the Arrhenius plot is used to determine the magnitude of the activation energy, which is represented by Figure 5. In the Arrhenius plot, the viscosity used on the Y-axis is the Francis-corrected viscosity. The Francis correction due to the wall effect is a constant in the form of a multiplier (K). It is on the logarithmic scale used in the Arrhenius plot. This multiplier has no impact on the gradient, as it only shifts the graph up or down. Graphic ln η versus 1/T on Figure 5, It can be seen that in general the value of ln η increases with increasing 1/T value. This indicates that fluid viscosity increases as temperature decreases, in accordance with the Arrhenius theory and the concept of fluid molecular kinetics. At high temperatures (small 1/T values), fluid molecules have greater kinetic energy so they move and slide more easily. As a result, the fluid viscosity becomes smaller. The curved shape of the plot line confirms systematic errors, one of which is caused by manual measurement of the ball's fall time.

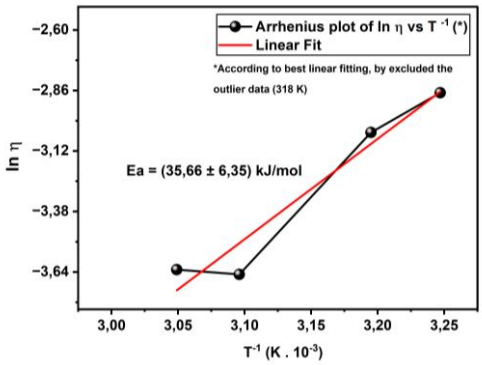

Figure 5 Linear Fitting of Arrhenius Plot of ln η versus 1/T to Evaluate Activation Energy

3.2.3 Uncertainty Analysis of Activation Energy from Arrhenius Law

As an analysis of the reliability of the Arrhenius law in representing the activation energy of the resulting data, the intercept, slope and activation energy parameters are used, which are described in Table 4. The activation energy is obtained through linearization of the Arrhenius equation from Figure 5. Through linear regression, the slope of the Arrhenius plot is (4.29 ± 0.76) kJ/mol. The activation energy is then calculated according to Eq. (5), so that the activation energy of Federal Racing Matic SAE 10W-30 oil is 35.66 ± 6.35 kJ/mol.

Table 4 Uncertainty of Intercept, Slope and Activation Energy

Parameter	Magnitude	Standard Error	% error
Slope (10^3)	4.29	0.76	17.7
Activation Energy (kj/mol)	35.66	6.35	17.8

3.2.4 Comparison of Activation Energy Data from Arrhenius Law Compared by Another Research

To evaluate the validity of the falling ball viscosity experimental device with manual time measurement using a stopwatch, a comparative analysis was conducted between the research data and the technical standard values of the TDS Federal Racing Matic SAE10W-30. Comparison of thermoviscosity parameters in activation energy is given in Table 5.

Table 5 Comparison of Activation Energy Data With other Research

Source	T (K)	Ea (kJ/mol)	Interpretation
Experiment	308 – 328	35,66 ± 6,35	-
(Puspitasari et al., 2024)	313 - 323	10,81	Unsuitable
(Calabokis et al., 2023)	300 -350	22 - 30	Almost suitable
(ExxonMobil Indonesia, 2025)	308 - 328	35,55	Suitable
(Canciam, 2012)	313 - 323	37,70	Suitable
(Hei et al., 2023)	313 - 328	39,44	Suitable

Oils with low viscosity and high viscosity index (such as type 10W-30) generally have an activation energy in the range of 22 kJ/mol – 30 kJ/mol at low to medium operating temperature s (Calabokis et al., 2023). Thus, the value of activation energy which obtained from this study is still within the reasonable range for lubricating oil or engine oil, which technically ranges from 20-50 kJ/mol, depending on the viscosity index (Ike, 2019). The E_a obtained (35.66 kJ/mol) is slightly lower when compared to heavy monograde engine oils such as SAE 40 (Tripathi & Vinu, 2015). This physically indicates that SAE 10W-30 has a lower energy resistance to flow, which is consistent with its nature as a thinner oil for fuel efficiency and engine protection during cold starts (ExxonMobil Indonesia, 2025).

3.3 Boltzmann Factor

Extracting the Boltzmann factor from thermo-viscosity requires a rigorous theoretical foundation; this section presents a conceptual derivation linking viscosity to molecular energy distribution. The phenomenon of viscous fluid flow can be explained by the Eyring Energy Transition Theory, which states that fluid can only flow if a molecular jump occurs from one state to the next. In laminar flow, each molecule is in its own state. The distance between states is λ_1 and the distance between molecules in equilibrium is λ. which prevents molecules from moving to another state. Molecules can only jump to the next state if they obtain energy greater than the potential barrier.

The initial state of the fluid molecules is in state 1 (Figure 6.a), in this state the net external force of the fluid molecular system is zero. In this initial state, macroscopically the fluid appears to be still but microscopically the molecular system performs random Brownian motion at a constant rate. When the ball is dropped into the fluid, the external force is not equal to zero, causing shear stress (τ). When τ has energy $E_{ext} > \epsilon_a$, it will do work W which makes the fluid molecules activated to transition by jumping over the potential wall between states at a speed v (Figure 6.b) whose direction is concentrated. The magnitude v is expressed by: $v = \lambda . k_{rate}$, where k_{rate} is the rate constant of molecular movement (microscopic) in the Eyring State Transition Theory.

Macroscopically, Newton's law of viscosity defines the relationship between τ with viscosity η and shear rate$\left(\frac{dv}{dx}\right)$ is $\tau = \eta \frac{dv}{dx} \approx \eta \frac{v}{\lambda_1} \approx \eta \frac{\lambda . k_{rate}}{\lambda_1}$, so that $\eta \approx \frac{\lambda_1 . \tau}{\lambda . k_{rate}}$. The work done by the shear force per molecule (W) is $W = \tau . \lambda_2 . \lambda_3 . \frac{\lambda}{2}$ where $\lambda_2 . \lambda_3$ s the effective area occupied by one fluid molecule. The net transfer rate towards state 2 becomes: $k_{net} = k_{rate}\left[\exp\left(\frac{W}{k_B T}\right) - \exp\left(-\frac{W}{k_B T}\right)\right] = 2k_{rate} . \sinh\left(\frac{W}{k_B T}\right)$. For Newtonian flow, the shear force is very small ($W \ll k_B T$) , so that with the Taylor series approach $\sinh(x) \approx x$, is obtained, so that the net fluid flow rate is: $k_{net} = 2k_{rate}\left(\frac{W}{k_B T}\right) = 2k_{rate}\left(\frac{\tau . \lambda_2 . \lambda_3 . \frac{\lambda}{2}}{k_B T}\right) = k_{rate}\left(\frac{\tau . \lambda_2 . \lambda_3 . \lambda}{k_B T}\right)$ which causes the viscosity can also be expressed as: $\eta = \tau \frac{\lambda_1}{\lambda} \frac{1}{k_{net}} = \frac{\lambda_1}{\lambda} \frac{1}{k_{rate}} \frac{k_B T}{(\tau . \lambda . \lambda_2 . \lambda_3)} = \frac{1}{k_{rate}} k_B T \frac{\lambda_1}{(\lambda^2 . \lambda_2 . \lambda_3)}$. By simplification, the term $\frac{\lambda_1}{(\lambda^2 . \lambda_2 . \lambda_3)}$ represents $\frac{1}{V_{molecular}}$ where $V_{molecular}$ is the volume for a single molecule, so that $\eta = \frac{k_B T}{V_{molecular}} . \frac{1}{k_{rate}}$.

While microscopically, the rate constant of molecular transport to jump over this energy barrier is fundamentally described by: $k_{rate} = \frac{n_2}{n_1} = \frac{k_B T}{h} K^{\ddagger}$ where n_2/n_1 is the molar ratio of the fluid fraction that successfully jumps from state 1 to state 2, $K^{\ddagger}$ is the quasi-equilibrium constant between the initial state and the activation state (Ramiasa et al., 2014). In chemical thermodynamics, $K^{\ddagger}$ is related to the Gibbs free energy in the activation process $\left(G^{\ddagger}\right)$, which is expressed by $K^{\ddagger} = \exp\left(-\frac{\Delta G^{\ddagger}}{RT}\right)$ dan $G^{\ddagger} = \Delta H^{\ddagger} - T\Delta S^{\ddagger}$, with $\Delta H^{\ddagger}$ is the activation enthalpy and $\Delta S^{\ddagger}$ is the activation entropy (Abramovič & Klofutar, 1998). So that the magnitude of k_{rate} becomes $k_{rate} = \frac{n_2}{n_1} = \frac{k_B T}{h} \exp\left(\frac{\Delta H^{\ddagger}}{RT}\right) \exp\left(-T\Delta S^{\ddagger}\right)$. Then viscosity is expressed by: $\eta = \frac{k_B T}{V_{molecular}} \frac{h}{k_B T} \exp\left(-\frac{(\Delta H^{\ddagger})}{RT}\right) \exp\left(\frac{T\Delta S^{\ddagger}}{RT}\right)$.

The Eyring equation reduces the group of parameters that are independent of temperature and groups the viscosity constant parameter as A, so that if it is written $\eta = A \exp\left(-\frac{\Delta H^{\ddagger}}{RT}\right)$. Then, by representing the activation enthalpy $\left(\Delta H^{\ddagger}\right)$ as the activation energy of fluid flow (E_a), the equation above becomes:

$\eta\ (T) = A \exp\left(-\frac{E_a}{RT}\right)$ where E_a is the amount of activation energy required to activate 1 mole of fluid fraction to transition to the next state (Haj-Kacem et al., 2014).

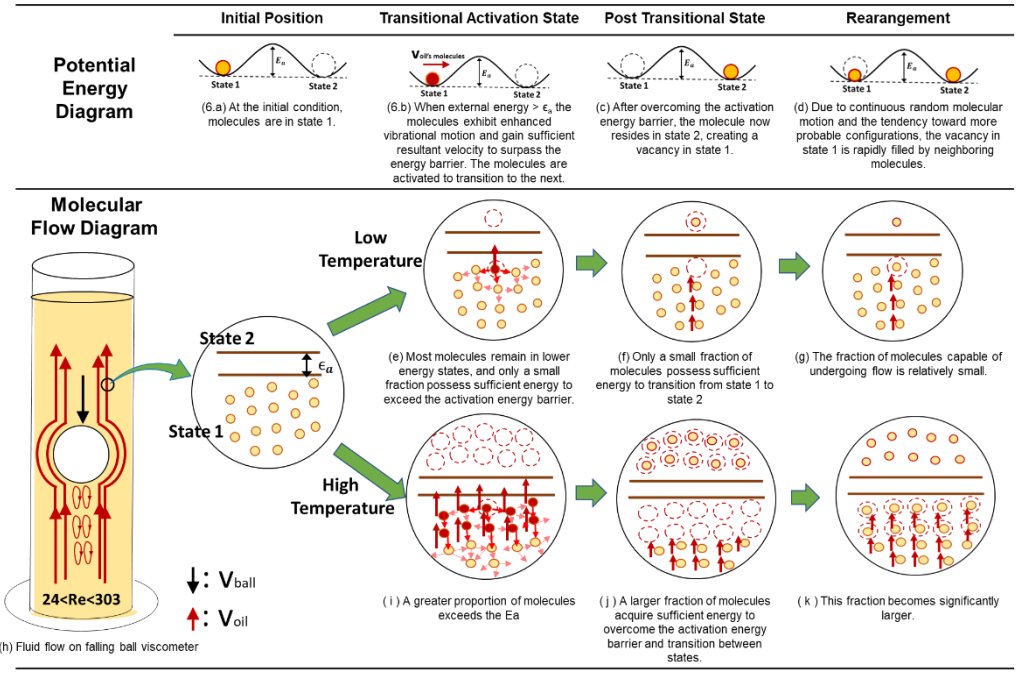

Figure 6 Molecular Distribution in Viscos Fluid

In molecular review, the magnitude of the activation energy per molecule (ϵ_a) is expressed by $\epsilon_a = \frac{E_a}{N_A}$. With the relationship between the Boltzmann constant (k_B) and the ideal gas constant (R) given by $k_B = \frac{R}{N_A}$, then: $\eta = A \exp\left(-\frac{\epsilon_a}{k_B T}\right)$. This equation is then used in the Arrhenius-Andrade viscosity model equation: $\ln \eta = -\frac{1}{T}.\frac{1}{k_B}.(-\epsilon_a) + Ln\ A$ (Andrade, 1930). By using the plot of the relationship between the x-axis is T^{-1} and the y-axis is the natural logarithm of viscosity $(\ln \eta)$ obtained from the experiment, the gradient of the linear regression (m) is obtained. Where this gradient determines the value of the activation energy per molecule (ϵ_a), which is $m = -\frac{\epsilon_a}{k_B}$.

After the molecule actively jumps the potential barrier, the molecule then occupies state 2 (Figure 6.c) and leaves a vacancy in state The flow rate of viscous fluid molecules in temperature variations can also be explained through Eyring's theory of Transitional State. When molecules are heated, energy absorption occurs which causes the molecules to jump "hopping" to the next state (Balázs, 1949). The higher the heating temperature (Figure 6.e), the more thermal energy the fluid molecules will obtain. This makes a larger fraction of molecules successfully jump from the potential wall (Figure 6.f). The greater the fraction of molecules, the greater the probability of molecules moving or flowing (Figure 6.g). However, at low temperatures, the thermal energy is relatively small which then reduces the number of molecules that can move (Figures 6.i - 6.k).

The ratio of molecules that successfully transition to the next state is expressed as the Boltzmann Factor. In statistical mechanics, the Boltzmann factor (P) is proportional to the exponential of the ratio of activation energy to absolute temperature or $P = C \exp\left(-\frac{\epsilon_a}{k_B T}\right)$ (Ozerov & Vorobyev, 2007). However, due to the limited accuracy of the exact viscosity values obtained, the accuracy of the Boltzmann Factor constant cannot be determined precisely. A strategic approach that can be taken is through the relative value of the Boltzmann Factor, which is expressed by Equation (6), where the reference temperature used is 313 K as the lowest reference data from TDS. In this study, after the ϵ_a value is obtained from

the slope, the relative Boltzmann factor value (P_{rel}) can also be obtained with a temperature (T) according to the interval 308 K – 328 K which is depicted in the yellow star symbol plot in Figure 7.

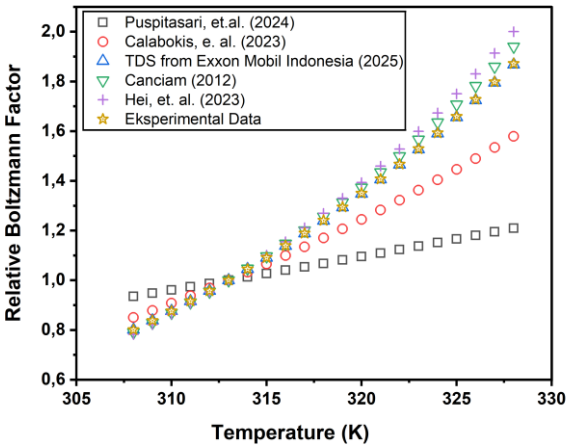

Figure 7 Relative Boltzmann Factor Comparison in SAE 30 Oil

The Boltzmann factor value increases monotonically with increasing fluid temperature. The probability of molecules being able to move at a temperature of 308K is 0.80, while at a temperature of 328K it is 1.87. At a temperature increase of 20K, the probability of molecules being able to move increases approximately 2 multiple times. This shows that the higher the fluid temperature, the greater the probability that molecules have enough energy to overcome the activation energy barrier. Molecularly, increasing temperature causes the average kinetic energy of fluid molecules to increase. Increasing temperature provides enough thermal energy for molecules to overcome the potential energy barrier (E_a) between layers of fluid (Fasina & Colley, 2008).

The experimental data (star markers) exhibit a trend that closely follows the literature curves, particularly those from TDS (ExxonMobil Indonesia, 2025), although slight deviations are observed at higher temperatures. However, it should be noted that TDS data are generally limited in detail, measurement conditions, and uncertainty reporting; therefore, additional comparisons with results from peer-reviewed studies remain necessary to ensure robustness and broader validation. The experimental data also overlapping with the results reported by Hei and Canciam, supporting the validity of the results (Canciam, 2012; Hei et al., 2023). Meanwhile, some references, such as (Calabokis et al., 2023; Puspitasari et al., 2024), show relatively lower values, reflecting variations in fluid formulation or measurement methods. No significant deviations are observed in the graph, indicating that the assumption of constant activation energy in this temperature range still holds. Thus, this Boltzmann factor analysis confirms the previous experimental results, namely that increasing temperature increases fluid molecule mobility and reduces viscosity.

3.4 Justification for The Feasibility of The Method as An Approach to Estimating the Boltzmann Factor

The feasibility of using the corrected falling ball viscometer method as an approach to estimate the Boltzmann factor is based on the theoretical bridge between the macroscopic resistance of the fluid and its microscopic molecular energy distribution. Through Arrhenius modelling, the activation energy obtained from experimental data of 35.66 kJ/mol becomes a key parameter to determine the fraction of molecules that have sufficient thermal energy to overcome the intermolecular interaction barriers. The statistical validity demonstrated by the coefficient of determination value $R^2 = 0.94$ provides strong positive correlation between viscocity and temperature, that justifies the Arrhenius-based in Boltzmann factor estimation. The dynamic viscosity values obtained through the Francis-corrected method with both industry Technical data Sheets and peer-reviewed lubricant studies (Table 1 and Table 5) and theoretical validation method (Section 3.3). The mean deviation of 25% between the experimental results and the literature benchmarks (Table 1) is primarily attributed to the high-blockage-ratio environment ($\lambda = 0.69$), where boundary-layer interactions are significantly more pronounced than in

standard industrial viscometry. The consistency of trends across datasets is a crucial point, as it demonstrates that despite differences in absolute values, the thermal behavior of the system remains preserved. Therefore, the Boltzmann factor derived from the experimental data is capable of representing the fundamental relationship between temperature and molecular energy distribution.

CONCLUSION

In conclusion, the viscosity measurements obtained in this study, although showing noticeable deviations from literature values even after Francis correction, are still able to capture a consistent and physically meaningful temperature-dependent trend. The presence of systematic limitations, including geometric confinement and experimental uncertainties, leads to the interpretation of the results as apparent viscosity rather than absolute values. However, this does not undermine the validity of the analysis, since the determination of activation energy and the Boltzmann factor relies primarily on the relative variation with temperature. The consistent increase of the relative Boltzmann factor with temperature further confirms that the viscous behavior of the system can be interpreted as a thermally activated process governed by molecular energy distribution. Therefore, the combined experimental and theoretical approach adopted in this study successfully provides a coherent link between macroscopic flow behavior and microscopic statistical mechanics, supporting the use of the Boltzmann framework in describing viscosity under non-ideal conditions. For further research, it is recommended that ball travel time measurements be conducted using digital measuring instruments or automatic sensors to improve data accuracy. Fluid temperature control should utilize a more stable heating system to minimize temperature fluctuations during measurement. Further research can also be conducted using different fluid types to compare the effect of temperature on viscosity and deepen the analysis of fluid flow activation energy.

ACKNOWLEDGEMENT

Thanks are due to the Universitas Kristen Indonesia, which has facilitated the Physics Education Laboratory, so that this research can be carried out.

REFERENCES

Abed, A. F., Hasan, H. A., & Abdul-Munaim, A. M. (2024). Refinement of Internal-Combustion Engine Oil Properties Via Magnetic Flux. *IOP Conference Series: Earth and Environmental Science*, *1371*(9), 092003. https://doi.org/10.1088/1755-1315/1371/9/092003

Abramovič, H., & Klofutar, C. (1998). Eyring Functions of Activation for the Viscous Flow of Some Higher Alcohols in Cyclohexane Solutions. *Monatshefte Für Chemie / Chemical Monthly*, *129*(8), 827–834. https://doi.org/10.1007/PL00013489

Andrade, E. N. D. C. (1930). The Viscosity of Liquids. *Nature*, *125*(3148), 309–310. https://doi.org/10.1038/125309b0

Ashley, A. W., Mookherjee, M., Xu, M., Yu, T., Manthilake, G., & Wang, Y. (2024). Viscosity Measurements at High Pressures: A Critical Appraisal of Corrections to Stokes' Law. *Journal of Geophysical Research: Solid Earth*, *129*(5), e2023JB028489. https://doi.org/10.1029/2023JB028489

Ataíde, C. H., Pereira, F. A. R., & Barrozo, M. A. S. (1990). Wall effects on the terminal velocity of spherical particles in Newtonian and non-Newtonian fluids. *Brazilian Journal of Chemical Engineering*, *16*, 387–394.

Atkins, P., & Paula, J. de. (2006). *Atkin's Physical Chemistry* (Eighth) [Book]. Oxford University Press.

Bachtiar, A., Aratri, R. P., & Ermawati, I. R. (2024). Penerapan Maxwell-Boltzman Pada Viskositas Berbasis Sensor Infrared. *Al-Irsyad Journal od Physics Education*, *3*(3). https://doi.org/https://doi.org/10.58917/ijpe.v3i2.119

Bai, B., Jin, H., Liu, P., Wang, W., & Zhang, J. (2022). Experimental study on the equilibrium position of a falling sphere in a circular tube flow. *International Journal of Multiphase Flow*, *153*, 104112. https://doi.org/10.1016/j.ijmultiphaseflow.2022.104112

Balázs, F. (1949). Theory of Viscosity. *Nature*, *164*(4161), 191–192. https://doi.org/10.1038/164191a0

Brewer, P. G., Peltzer, E. T., & Lage, K. (2021). Life at low Reynolds Number Re-visited: The apparent activation energy of viscous flow in sea water. *Deep Sea Research Part I: Oceanographic Research Papers*, *176*, 103592. https://doi.org/10.1016/j.dsr.2021.103592

Calabokis, O. P., Nuñez De La Rosa, Y., Ballesteros-Ballesteros, V., Borges, P. C., & Cousseau, T. (2023). Effect of a Metal Conditioner on the Physicochemical Properties and Tribological Performance of the Engine Oil SAE 5W-30 API SN. *Lubricants*, *11*(7), 305. https://doi.org/10.3390/lubricants11070305

Calabokis, O. P., Nuñez De La Rosa, Y., Borges, P. C., & Cousseau, T. (2022). Effect of an Aftermarket Additive in Powertrain Wear and Fuel Consumption of Small-Capacity Motorcycles: A Lab and Field Study. *Lubricants*, *10*(7), 143. https://doi.org/10.3390/lubricants10070143

Canciam, C. (2012). Estimativa da energia de ativação de fluxo dos óleos lubrificantes SAE 30, SAE40 e SAE 50. *Revista da Universidade Vale do Rio Verde*, *10*(2), 202–210. https://doi.org/10.5892/ruvrv.2012.102.202210

Celata, G. P., Cumo, M., McPhail, S., & Zummo, G. (2006). Characterization of fluid dynamic behaviour and channel wall effects in microtube. *International Journal of Heat and Fluid Flow*, *27*(1), 135–143. https://doi.org/10.1016/j.ijheatfluidflow.2005.03.012

Chekirda, K. V., Demyanov, A. A., Nekliudova, A. A., Domostroev, A. V., & Sulaberidze, V. Sh. (2022). State Primary Standards of Density and Dynamic and Kinematic Liquid Viscosities: History of Creation and Modernization. *Measurement Techniques*, *65*(7), 487–492. https://doi.org/10.1007/s11018-023-02108-w

Cho, Y. I., Hartnett, J. P., & Kwack, E. Y. (1980). *A Study of Wall Effect for Viscoelastic Fluids in The Falling Ball Viscometer* (Pt. 141-149). *6*((1-3)). https://doi.org/https://doi.org/10.1080/00986448008912526

ExxonMobil Indonesia. (2025). *Federal Racing Matic 10W-30 Pelumas Kendaraan Penumpang, Indonesia* (Oli Mesin Skuter Empat Tak Berkinerja Tinggi) [Pdf]. https://federaloil.co.id/product-detail/170121/Federal-Racing-Matic-10W-30

Fasina, O. O., & Colley, Z. (2008). Viscosity and Specific Heat of Vegetable Oils as a Function of Temperature: 35°C to 180°C. *International Journal of Food Properties*, *11*(4), 738–746. https://doi.org/10.1080/10942910701586273

Fazio, C., Battaglia, O. R., & Guastella, I. (2012). Two experiments to approach the Boltzmann factor: Chemical reaction and viscous flow. *European Journal of Physics*, *33*(2), 359–371. https://doi.org/10.1088/0143-0807/33/2/359

Gorban, A. N., & Tyukin, I. Y. (2018). Blessing of dimensionality: Mathematical foundations of the statistical physics of data. *Philosophical Transactions of the Royal Society A: Mathematical, Physical and Engineering Sciences*, *376*(2118), 20170237. https://doi.org/10.1098/rsta.2017.0237

Guisasola, J. (2014). Teaching and Learning Electricity: The Relations Between Macroscopic Level Observations and Microscopic Level Theories. In M. R. Matthews (Ed.), *International Handbook of Research in History, Philosophy and Science Teaching* (pp. 129–156). Springer Netherlands. https://doi.org/10.1007/978-94-007-7654-8_5

Haj-Kacem, R. B., Ouerfelli, N., Herráez, J. V., Guettari, M., Hamda, H., & Dallel, M. (2014). Contribution to modeling the viscosity Arrhenius-type equation for some solvents by statistical correlations analysis. *Fluid Phase Equilibria*, *383*, 11–20. https://doi.org/10.1016/j.fluid.2014.09.023

Hamdi, R., & Mliki, E. (2023). Correlation analysis of the relationship between Arrhenius viscosity parameters in Binary Liquid Mixtures. *South African Journal of Chemical Engineering*, *43*, 337–341. https://doi.org/10.1016/j.sajce.2022.12.002

Haryanto, A., & Prabawa, S. (2016). *Kinetika Sintesis Biodiesel Dari Minyak Jelantah Dengan Metode Transesterifikasi Basa yang Diperkuat Gelombang Mikro dan Gelombang Ultrasonik* (Laporan Akhir Penelitian Fundamental 163/Teknologi Pertanian). Universitas Lampung.

Hei, D., Zheng, M., Liu, C., Jiang, L., Zhang, Y., & Zhao, X. (2023). Study on the frictional properties of the top ring-liner conjunction for different-viscosity lubricant. *Advances in Mechanical Engineering*, *15*(2), 16878132231155002. https://doi.org/10.1177/16878132231155002

Hull, M. M., Jansky, A., & Hopf, M. (2021). Probability-related naïve ideas across physics topics. *Studies in Science Education*, *57*(1), 45–83. https://doi.org/10.1080/03057267.2020.1757244

Ike, E. (2019). The study of viscosity-temperature dependence and activation energy for palm oil and soybean oil. *Global Journal of Pure and Applied Sciences*, *25*(2), 209–217. https://doi.org/10.4314/gjpas.v25i2.11

Iwaoka, M., & Ishii, T. (1979). Experimental wall correction factors of single solid spheres in circular cylinders. *Journal Of Chemical Engineering Of Japan*, *12*(3), 239–242. https://doi.org/10.1252/jcej.12.239

Jovanovick, F., & Schinckus, C. (2018). *Breaking Down The Barriers Between Econophysics and Financial Economics*. https://ssrn.com/abstract=3294553

Karmakar, S., Lerner, E., & Procaccia, I. (2010). Statistical Physics of the Yielding Transition in Amorphous Solids. *Physical Review E*, *82*(5), 055103. https://doi.org/10.1103/PhysRevE.82.055103

Khan, M., Choudhary, F. R., & Ali, M. (2025). *A Quantitative Study of Cognitive, Affective, and Instructional Barriers to Learning Physics at the College Level*. *8*(4), 1–9. https://doi.org/10.36902/sjesr-vol8-iss4-2025(1-9)

Khan, S. U., Usman, Al-Khaled, K., Hussain, S. M., Ghaffari, A., Khan, M. I., & Ahmed, M. W. (2022). Implication of Arrhenius Activation Energy and Temperature-Dependent Viscosity on Non-Newtonian Nanomaterial Bio-Convective Flow with Partial Slip. *Arabian Journal for Science and Engineering*, *47*(6), 7559–7570. https://doi.org/10.1007/s13369-021-06274-3

Koerfer, E. (2025). *Conceptual reasoning, intuition, and mathematics in physics: Statistical mechanics as a starting point for exploring student reasoning in upper-level university courses* [Licentiate thesis, comprehensive summary, Uppsala University]. DiVA. http://urn.kb.se/resolve?urn=urn:nbn:se:uu:diva-555837

Lang, J. (2012). *Comparative Study of Hands-on and Remote Physics Labs for First Year University Level Physics Students*. *6*(1).

Miller, J. N., & Miller, J. N. (2010). *Statistics and Chemometrics for Analytical Chemistry* (Sixth) [Book]. Pearson. https://repo.upertis.ac.id/1924/1/Statistik.pdf

Montgomery, D. C., & Runger, G. C. (2018). *Applied Statistics And Probability For Engineers* (7th ed.). Wiley. https://lccn.loc.gov/2017043465

Mushtaq, Z., & Hanief, M. (2021). Evaluation of Tribological Performance of Jatropha Oil Modified With Molybdenum Disulphide Micro-Particles for Steel–Steel Contacts. *Journal of Tribology*, *143*(2), 021401. https://doi.org/10.1115/1.4047752

Ozerov, R. P., & Vorobyev, A. A. (2007). 3—Molecular Physics. In *Physics for Chemists* (pp. 169–250). Elsevier. https://doi.org/10.1016/B978-044452830-8/50005-2

Puspitasari, P., Permanasari, A. A., Habibi, I. A., & Pramono, D. D. (2024). *A comparative study on stability, thermal conductivity, and rheological properties of nanolubricant using carbon-based additive*.

Ramiasa, M., Ralston, J., Fetzer, R., & Sedev, R. (2014). The influence of topography on dynamic wetting. *Advances in Colloid and Interface Science*, *206*, 275–293. https://doi.org/10.1016/j.cis.2013.04.005

Rhodes, M., & Seville, J. (2024). *Introduction to particle technology* (3rd ed.). (Original work published John Wiley & Sons)

Rosen, D. J., & Kelly, A. M. (2020). Epistemology, socialization, help seeking, and gender-based views in in-person and online, hands-on undergraduate physics laboratories. *Physical Review Physics Education Research*, *16*(2), 020116. https://doi.org/10.1103/PhysRevPhysEducRes.16.020116

Salim, M. B. (2014). Mengetahui Pengaruh Koefisien Viskositas Akuades Terhadap Variasi Diameter Tabung Menggunakan Adobe Audition 1.5. *Jurnal Pendidikan Fisika*, *2*(2). https://doi.org/10.24127/jpf.v2i2.121

Schlichting, H., & Gersten, K. (2017). *Boundary-Layer Theory*. Springer Berlin Heidelberg. https://doi.org/10.1007/978-3-662-52919-5

Shams, M., & Mirzaie, M. A. (2025). Statistical Inference and Simulation for the Maxwell-Boltzmann Distribution. *Advanced Theory and Simulations*, *8*(9), 2500148. https://doi.org/10.1002/adts.202500148

Southard, J. (2019). Introduction to Fluid Motions and Sediment Transport. In *Introduction to Fluid Motion and Sedimen Transport: Https://geo.libretexts.org/@go/page/5658*. LibreTexts. (Original work published Massachusetts Institute of Technology)

Suharto., T. E. (2022). *Katalisis dalam Industri Kimia* (1st ed.). UAD PRESS.

Suri, P., Patel, S. A., & Chhabra, R. P. (2023). Falling ball method for determining zero shear and shear-dependent viscosity of polymeric systems: Solutions, melts, and composites. *Journal of Vinyl and Additive Technology*, *29*(4), 670–684. https://doi.org/10.1002/vnl.21966

Swendsen, R. H. (2012). *An Introduction to Statistical Mechanics and Thermodynamics*. Oxford University Press.

Taha, M., M. Mousa, H., Alfadhel, H., Abouel Nasr, E., Elbatran, A. H. A., Nabhan, A., & R. El-Sharkawy, M. (2024). Utilizing cellulose nanofibers to enhance spent engine oil performance: A sustainable environmental solution. *Results in Engineering*, *23*, 102395. https://doi.org/10.1016/j.rineng.2024.102395

Trevor, I., John, R. T., & Donald, B. M. (2010). Addressing Student Difficulties with Statistical Mechanics: The Boltzmann Factor. *AIP Conference Proceeding*, *1289*(1). https://doi.org/https://doi.org/10.1063/1.3515230

Tripathi, A. K., & Vinu, R. (2015). Characterization of Thermal Stability of Synthetic and Semi-Synthetic Engine Oils. *Lubricants*, *3*(1), 54–79. https://doi.org/10.3390/lubricants3010054

Truesdell, C., & Rajagopal, K. R. (2000). *An Introduction to the Mechanics of Fluids*. Birkhäuser Boston. https://doi.org/10.1007/978-0-8176-4846-6

Wentao, H., Zifeng, Z., Zhitao, Z., & Feipeng, X. (2024). Modification and Application of the Arrhenius Equation Based on Activated Energy Methods from Various Asphalt Binders. *Journal of Materials in Civil Engineering*, *36*(6), 04024123. https://doi.org/10.1061/JMCEE7.MTENG-17482

Xue, J., Nogueira, F. S., Kelton, K. F., & Nussinov, Z. (2022). Deviations from Arrhenius dynamics in high temperature liquids, a possible collapse, and a viscosity bound. *Physical Review Research*, *4*(4), 043047. https://doi.org/10.1103/PhysRevResearch.4.043047

Zanoun, E.-S., Bauer, C., Wagner, C., Durst, F., Egbers, C., Bellani, G., & Talamelli, A. (2025). Cross-validation of numerical and experimental data in turbulent pipe flow with new scaling correlations. *Journal of Turbulence*, *26*(8–9), 251–272. https://doi.org/10.1080/14685248.2025.2560314